

A STUDY OF THE COLLISIONLESS INTERACTION OF
INTERPENETRATING SUPER-ALFVÉN PLASMA FLOWS

V. M. Antonov, V. P. Bashurin, A. I. Golubev,
V. A. Zhmailo, Yu. P. Zakharov, A. M. Orishich,
A. G. Ponomarenko, V. G. Posukh, and V. N. Snytnikov

UDC 533.95

Introduction. Various phenomena observed in space plasma such as outbursts from supernovae [1] involve the ejection of plasma clouds, as do certain experiments in space [2, 3], which are heavily retarded in the surrounding magnetized plasma on scale much less than the characteristic ion mean free paths. Such collisionless interaction effects may be important also in magnetic gas-projection methods for the first wall in a fusion reactor with inertial containment [4].

At the high expansion velocities typical of such clouds, namely $v_0 \approx 10^7$ - 10^8 cm/sec, and in the presence of a background plasma with ion concentration n_* and mass m_2 in a field B_0 , the motion of the cloud is substantially super-Alfvén $M_A = v_0 \sqrt{4\pi n_* m_2} / B_0 \gg 1$. However, there were no reliable experimental data until recently [5] for large Mach-Alfvén numbers M_A to confirm the possibility of collisionless interaction between mutually penetrating plasma fluxes in a transverse magnetic field.

Theoretical calculations show that energy-transfer mechanisms related to the formation of a longitudinal electric field (along v_0) at the boundary between the fluxes [6] becomes ineffective as M_A increases, as does the mechanism associated with anomalous friction due to the occurrence of two-flux instabilities [7].

In [8, 9], a study was made of the scope for collisionless interaction between super-Alfvén fluxes due to a magnetic laminar mechanism (MLM) independent of M_A [10]. The energy exchange between the fluxes in that case is via the transverse vortical electric field $(E_{\theta} \perp B_0, v_0)$, which arises in a layer at the leading edge of the cloud, which displaces the magnetic field from its volume. Estimates and numerical calculations [9-11] show that a spherical cloud containing N_1 ions of mass m_1 and mean charge z_1 provides an energy-exchange performance from this mechanism that is entirely determined by the interaction parameter $\delta = R_*^2 / R_1 R_2$, where $R_* = (3N_1 z_1 / 4\pi n_*)^{1/3}$ is the characteristic radius for the displacement of the magnetic field by the cloud, while R_1 and R_2 are the Larmor radii of the ions in the cloud and background, which are defined by the initial field B_0 and the mean mass velocity $v_1 = (2W_0 / N_1 m_1)^{1/2}$ of the cloud with energy W_0 . In particular, for $\delta \gg 1$ the cloud may lose much of its initial energy in a distance $R_m = (3N_1 m_1 / 4\pi n_* m_2)^{1/3}$.

Although there are numerous experiments on the interaction of magnetized plasma fluxes, only a few of them have [10] been performed at high Mach numbers ($M_A \gtrsim 5$) and under conditions excluding collisional effects. It is complicated to examine the magnetic laminar mechanism at high Mach numbers because of the severe specifications for the plasma sources: one needs cloud and background plasmas with near-record parameters: $N_1 \gtrsim 10^{18}$ particles, $v_0 \approx (3-5) \cdot 10^7$ cm/sec, and $n_* \sim 10^{14}$ cm $^{-3}$ (at a background temperature $T_e \approx 5-10$ eV) in a volume $\gtrsim 1$ m 3 [10]. Parameters close to these have been obtained only in the Nimbus-II experiment [12], in which a precursor for the plasma cloud occurred at $\delta \approx 0.1$.

In our experiments [13] on collisionless interaction at $M_A \approx 10-20$ and with the MLM switched out ($\delta < 10^{-3}$), we observed free expansion of the cloud in the background plasma at distances up to $4R_m$, and therefore we obtained reliable experimental evidence for the absence of any plasma-flux interaction mechanism at $M_A \gg 1$ and $\delta \ll 1$. In [5] it was found that a plasma cloud expanding in an axially symmetry fashion with respect to the field B_0 effectively displaces it out to a distance R_* , in accordance with the model for exchange between magnetized electron components in the cloud and background [8], which thus provided the vortex electric fields required for the MLM.

Novosibirsk. Translated from Zhurnal Prikladnoi Mekhaniki i Tekhnicheskoi Fiziki, No. 6, pp. 3-10, November-December, 1985. Original article submitted December 7, 1984.

The purpose of the present study was to attain plasma parameters as required for effective MLM interaction, while examining the collisionless interaction of an expanding laser-plasma cloud with a magnetized background for $M_A \gtrsim 5$ and $\delta \gtrsim 1$.

1. Apparatus. The experiments were performed with the KI-1 apparatus [13, 14] for simulating astrophysical plasma processes. The main components were the 1-kJ CO₂ laser [15] and a high-vacuum chamber of diameter 1.2 m and length 5 m fitted with a pulsed background-plasma source. Figure 1 shows the general scheme, with the central (main) section of the chamber, at the center of which is the target 1, and in the plane of it are the diagnostic components 2-5 for examining the expansion of the cloud in the background 6 in directions perpendicular to B_0 .

A cloud with nearly spherical symmetry was produced by irradiating a 0.25 mm diameter filament with two beams from a CO₂ amplifier incident on opposite sides along almost radial directions. The capron filament (C₆H₁₁ON)_n was oriented along the axis of the chamber and the magnetic field B_0 . The filament was suspended at the center from a glass capillary and was adjusted relative to the beams via the window 7 with an accuracy of about 0.1 mm. A special mirror system 8 focused the radiation to a diameter of about 4 mm in the region of the target. As the beam diameters were more than 10 times greater than the filament diameter, and as the filament was bombarded from both sides, axial symmetry was produced in the plasma flow in a plane perpendicular to the filament not only as regards the mean velocity (deviations not more than $\pm 7\%$) but also as regards the number of particles $dN_1/d\Omega$ in the flux ($\pm 10\%$). The good axial symmetry in the plane perpendicular to B_0 is evident from the image-converter picture (Fig. 2) showing the emission in vacuum ($n_x = 0$) for $B_0 = 0$ at $t = 1.65$ μ sec after the laser pulse, as well as from control experiments on the expansion in a magnetic field for $n_x = 0$.

We have shown for this case [16] that such a cloud displaces B in the manner of an expanding superconducting sphere whose skin-layer thickness is close to the collisionless value within a distance $R < R_0 \approx (3W_0/B_0^2)^{1/3}$, which is the theoretical deceleration radius for the cloud for $n_x = 0$ [17].

The free expansion ($n_x = 0$, $B_0 = 0$) was of self-modulating type: the ion speed at a distance R from the target at time t was $v = R/t$. This was confirmed not only by the law of motion ($R \sim t$) for the maximal density of the radial ion current j_r but also by the dependence $j_r \sim R^{-3}$ with which the maximum fell at distances $15 \leq R \leq 250$ cm. The cloud consisted in the main of 55% H⁺, 30% C⁴⁺, and 15% C³⁺. With a pulse energy at the target of 400 J, a typical flux was produced with $v_0 \approx 2.3 \cdot 10^7$ cm/sec (see the $j_r(t)$ signal at $R = 40$ cm, curve 1 in Fig. 3a), which contained $N_1 \approx (8 \pm 1.5) \cdot 10^{17}$ ions and had total energy $W_0 = 45 \pm 7$ J.

The background plasma was provided by a separate source at the end of the chamber, which enabled us to provide a plasma homogeneous over a volume of about 1.5 m³ with known and adjustable parameters. The source was an induction generator based on IK 50-3 capacitors. The plasma was produced by ionizing the gas (hydrogen, nitrogen, argon, etc.) emitted as a pulse into a ceramic tube of diameter 20 cm and transported over a distance of about 3 m into the principal section of the chamber, where it expanded to a characteristic diameter of 90 cm in the magnetic nozzle at the exit from the source. The maximum ion concentration in the hydrogen background in the principal section was $n_x \approx 6 \cdot 10^{13}$ cm⁻³ with $T_e \approx 10$ eV. Typical initial distributions for $n_x(R)$ and $B_0(R)$ are shown by the dashed lines in Fig. 4 (points 1). The variation in B_0 with R is due to the background plasma being diamagnetic. With $B_0 = 0$, the plasma concentration in the target zone was up to $n_x \approx 3 \cdot 10^{13}$ cm⁻³. The vacuum volume was evacuated by magnetic-discharge pumps. The residual gas pressure was not more than 2.7×10^{-4} Pa.

Figure 1 shows the disposition of the principal components. The double probes 2 were used to measure T_e and n_e , while the ion-flux collectors 3 and 4 were used to measure the fluxes in the radial direction j_r and the azimuthal one $j_{\phi \perp B_0}$, v_0 , while the magnetic probes 5 were used to record ΔB for the axial component of B_0 . Special multichannel cable inputs of the type of 3 and 5 were used in the flanges in the principal section to mount several sensors in each radial direction, which provided data on the dynamics of the interaction at various distances from the target in various directions in a single experiment, with the plasma cloud expanding transversely to B_0 . In special check experiments, it was found that the diagnostic equipment had no effect on the physical process.

The ion composition of the cloud was determined by means of a time-of-flight analyzer as briefly described in [18]. In some experiments, the emission from the cloud was

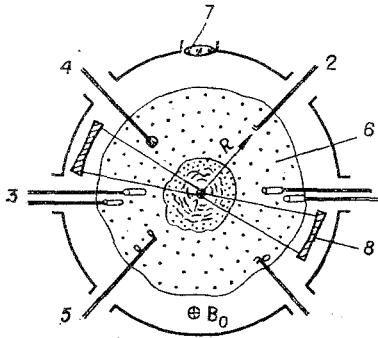


Fig. 1

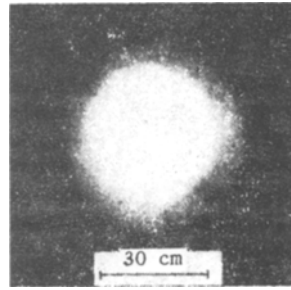


Fig. 2

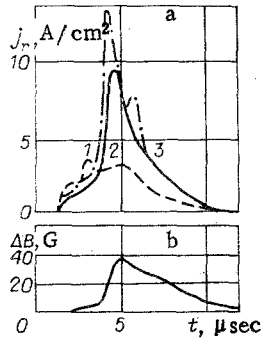


Fig. 3

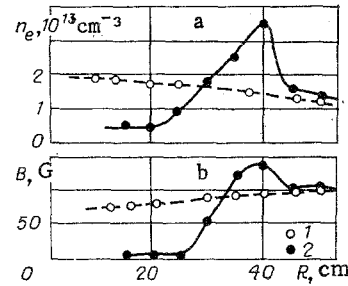


Fig. 4

recorded with an EOC of LV-05 type along the chamber axis. All the recording equipment had time resolution better than 50 nsec, while the circuits for the contact diagnosis were protected from possible interference by the cloud potential (up to 500 V).

2. Results. Particular attention was given to eliminating the effects from ordinary Coulomb collisions, which can produce appreciable momentum transfer and can thus cause the background to move if $\lambda \gg R_m$, where λ is the mean free path of an ion from the cloud in the background. By analogy with [19], we examined various forms of collisional interaction, including the Coulomb one, screened nuclear repulsion, polarization-type attraction, and charge transfer, which showed that under our conditions with a hydrogen background, the minimum mean free path ($\lambda_m \approx 210$ cm) for the cloud ions as determined from the momentum loss was governed by multiple ion-ion Coulomb collisions. In the experiments with an argon background plasma, the mean free path ($\lambda_m \approx 120$ cm) was less because of repeated ion-electron Coulomb collisions involving cold background electrons ($T_e = 2$ eV). However, in all cases the minimal values λ_m exceeded the characteristic dimensions of the equipment $R_c = 60$ cm, as is evident from the parameters given in Table 1. An important point is that the performance in ion-ion scattering is independent of B_0 , whereas for ion-electron collisions there is an indirect effect of B_0 via the Joule electron heating, which may increase λ_m . The main method in the experiment was that the MLM was switched in by increasing the magnetic field while maintaining $\lambda \approx \text{const}$ ($n_* \approx \text{const}$), measurements being made on the effects on the radial flux j_r and the azimuthal one j_ϕ , as well as the radial concentration distribution.

It was found that with a hydrogen background plasma having $n_* \lesssim 10^{13} \text{ cm}^{-3}$, magnetic fields in the range $0 \leq B_0 \leq 250$ G did not affect the cloud motion on a scale $R \lesssim 40$ cm; for $n_* \gtrsim 2 \cdot 10^{13} \text{ cm}^{-3}$, B_0 began to have an effect at values $B_0 > 50$ G in that j_r was modified at $R \gtrsim 30$ cm. The $j_r(t)$ waveforms at $R = 40$ cm for $n_* = 2 \cdot 10^{13} \text{ cm}^{-3}$ (Fig. 3a) show that when B_0 is switched on (curve 2), there is retardation in the fast leading part of the cloud, i.e., there is retardation in the fast leading part of the cloud, i.e., there is a reduction in the number of ions having velocities of $2.5-1 \times 10^7$ cm/sec, while at the same time there is an increase in the intensity of the flux moving with the relatively low mean velocity (5×10^6 cm/sec). A plasma layer of 10-15 cm thickness is formed that moves together with the magnetic piston (Fig. 3b shows $\Delta B(t)$). The value of j_r in the layer considerably exceeded the flux in the plasma cloud for $B_0 = 0$ (curve 1). The main regularities in the propagation

TABLE 1

Background plasma com- position	N_1	W_0 , J	v_0 , cm/ sec	v_1 , cm/sec	n_* , cm ⁻³	T_e , eV	B_0 , G	λ_m , cm		$M_A = \frac{v_0}{v_0 \sqrt{4\pi n_1 n_2}}$ B_0	R_0 , cm	R_{th} , cm (theory/ expt.)	$\delta = \frac{R_{th}^2}{R_1 R_2}$	R_m , cm (theory/ expt.)
								H ⁺	C ⁺³					
H ⁺	$8 \cdot 10^{17}$	45	$2,3 \cdot 10^7$	10^7	$(2-4) \cdot 10^{13}$	40	75	210 *	300 *	6-10	62	$\frac{24-28}{30-35}$	1-1,6	$\frac{40-50}{30-40}$
Ar ⁺	$4,3 \cdot 10^{17}$	40	$2,6 \cdot 10^7$	10^7	$2 \cdot 10^{13}$	2	100	124 †	170 †	30	50	$\frac{25}{25}$	$2 \cdot 10^{-2}$	$\frac{12}{-}$

*Repeated Coulomb scattering at ions with $v = 1.3 \times 10^7$ cm/sec.

†Repeated Coulomb scattering at electrons.

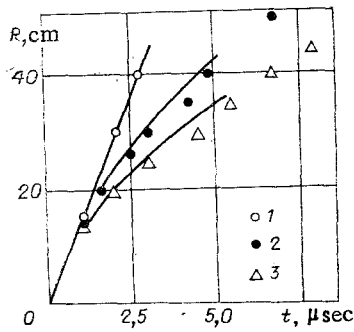


Fig. 5

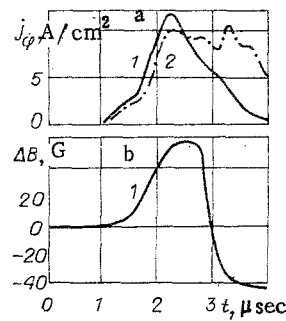


Fig. 6

of this layer are illustrated by the R - t diagram for the maximum in the flux, as shown in Fig. 5, where points 1 represent the state with $B_0 = 0$, $n_{*} = 2 \cdot 10^{13} \text{ cm}^{-3}$, 2) $B_0 = 75 \text{ G}$, $n_{*} = 2 \cdot 10^{13} \text{ cm}^{-3}$, 3) $B_0 = 65 \text{ G}$, $n_{*} = 4 \cdot 10^{13} \text{ cm}^{-3}$. It is evident that the interaction of the cloud with the background at $B_0 = 75 \text{ G}$ makes itself felt in plasma retardation, i.e., a reduction in the characteristic velocity from 1.3×10^7 at $R = 15 \text{ cm}$ to $5 \times 10^6 \text{ cm/sec}$ at $R = 40 \text{ cm}$ ($n_{*} = 2 \cdot 10^{13} \text{ cm}^{-3}$). As n_{*} increases, the speed of this plasma layer decreases as $\sim n_{*}^{-1/2}$.

The total number of particles transferred outside a sphere of radius $R = 30 \text{ cm}$ was equal within the $\pm 20\%$ measurement-error limits to the total number of particles in the cloud and background within that sphere. Consequently, the magnetic field produced a radial acceleration in the background plasma to the speed of the cloud and virtually complete displacement from the region $R \lesssim 30 \text{ cm}$.

This conclusion is confirmed by measurements on the plasma distribution given in Fig. 4a (points 2). At $t = 5.8 \mu\text{sec}$, the cloud and background are localized in a region bounded by the radii $35 \lesssim R \lesssim 45 \text{ cm}$. The background motion is uniquely related to the displacement of the magnetic piston (region $B > B_0$ in Fig. 4b, points 2), while the steady-state $n_e(R)$ distribution is related to the formation of the magnetic cavity, as is evident from parts a and b of Fig. 4 (region $0 \leq B < B_0$ in Fig. 4b).

We recorded anisotropic j_ϕ in a hydrogen background, which accompanied the motion of the magnetic piston at $R = 10$ - 30 cm ; these are shown in Fig. 6 as $j_\phi(t)$ (curve 1) and $\Delta B(t)$ oscillograms for the case $B_0 = 75 \text{ G}$ and $n_{*} = 2 \cdot 10^{13} \text{ cm}^{-3}$. At large distances ($R > 30 \text{ cm}$), one gets an azimuthal flux in the reverse direction, which corresponds to the motion of the cloud ions in the magnetic field.

As the mass of the background ions increased at a constant electron concentration $n_{*} = 2 \cdot 10^{13} \text{ cm}^{-3}$ for a field $B_0 \approx 100 \text{ G}$, the interaction ceased; for example, while a perturbation in n_{*} could still be observed for a nitrogen background plasma, we did not find any change in the density of an argon plasma, or any perturbations in the radial cloud ion flux on a scale $R \lesssim 40 \text{ cm}$.

3. Interaction Type: Comparison with Theory. We first characterize the basic parameters for the collisionless interaction of an expanding laser-plasma cloud with a magnetized hydrogen background under the conditions of our experiment, which are given in Table 1.

In the absence of the background plasma, the limiting field-displacement radius (radius of the magnetic cavity) was the same as the retardation radius for a field $B_0 = 75 \text{ G}$, which should be $R_0 \approx 62 \text{ cm}$ [17]. The size of the magnetic cavity in the background for $n_{*} \approx (2-4) \cdot 10^{13} \text{ cm}^{-3}$ should be $R_{*} \approx 22$ - 28 cm . However, the interaction due to the motion of the background causes the actual R_{*} to be 30 - 35 cm . In that case, the cloud loses only a small proportion of its energy in displacing B_0 ($\xi_1 = \Delta W/W_0 \approx (R_{*}/R_0)^3 \approx 0.11$ - 0.18).

At the same time, the value $\delta \approx 1$ - 1.6 is sufficiently large for the expected proportion of the cloud energy [11] transferred to the background on a scale $R_m \approx 40$ - 50 cm by the magnetic laminar mechanism to be substantial ($\xi_2 \approx 0.35\delta \approx (0.3$ - $0.6)$); the value of M_A was about 6 - 10 , being determined by the speed v_0 of the leading edge of the cloud.

Therefore, estimates for a hydrogen background show that conditions are realized for the cloud to be retarded by the background via MLM interaction involving the vortical electric field.

In accordance with the MLM, the radial and azimuthal motions of the background plasma are uniquely related to the formation of a magnetic cavity and the propagation of the field compression (Figs. 3, 4, and 6). Also, check experiments showed that the interaction performance is substantially dependent on δ . For $\delta < 0.2$, the interaction ceases at a scale of $R \approx 40$ cm, and the result is independent of the method of adjusting this parameter. A reduction can be produced by increasing the mass of the background ions to $m_2 = 40$ amu for $B_0 \approx$ const or by changing the magnetic field. In particular, with an argon background (parameters given in Table 1), no motion in the background plasma was observed, and the cloud can dissipate energy only by deforming the magnetic field. The perturbation in the radial flux at $R \leq 40$ cm in that case did not exceed the observed spread in j_r (about 15%) with the cloud expanding under vacuum ($n_* = 0$ and $B_0 = 0$). Therefore, this experiment showed that there is only comparatively small energy loss from the laser plasma in producing the magnetic cavity.

A more detailed study was made of the scope for describing the observed transfer from the cloud to the background by the magnetic laminar mechanism by means of a numerical simulation performed with a two-dimensional hybrid model [9, 11].

We derived the initial velocity distributions for the various ionic components at $t = 0$ on the basis of the self-modeling type of expansion, where an analyzer was used to identify the partial ion currents j_r^k for ions of type k , which were identified from m_k and z_k via the known target composition. These data on $(m/z)_k$ and j_r^k were derived at $R = 250$ cm and $n_* = 0$ and $B_0 = 0$ by the use of ion cutoff at energies $m_k v_k^2 / 2 \leq z_k e \varphi_k$ produced by a retarding potential φ in the analyzer in conjunction with time-of-flight measurement of the velocity $v_k = R/t_k$ [18]. The background hydrogen plasma was defined as having an inhomogeneous radial distribution $n_*(R)$ analogous to that actually observed (Fig. 4a). At the boundary $R_k = 60$ cm, conditions were defined for the magnetic field not to penetrate (ideally conducting wall) and for complete particle absorption.

Figure 3a shows the results as the density of the total radial ion current j_r . The calculated j_r (curve 3) may be compared with the measured value (curve 2); there is good agreement not only as regards signal arrival time but also amplitude (the difference in the maximum does not exceed 40%). The numerical simulation showed that this peak in j_r is due to extensive entrainment of the background plasma in the motion for $\delta \gtrsim 1$, while the non-monotone fall in $j_r(t)$ after this maximum is related to some features in the numerical simulation of the background motion in such complicated two-dimensional cases. Figure 5 shows R-t diagrams for the motion of the maximum in j_r constructed from the calculated results (solid lines) and from the corresponding experimental data, not only for the expansion of the cloud in the background without retardation (points 1, $B_0 = 0$) but also in the presence of interaction (points 2 and 3, $B_0 \neq 0$). The numerical simulation data for the radial motion are in good agreement with the measurements out to $R \approx 40$ cm.

The calculations enabled us to follow the energy transfer in the cloud-field-background system in some detail. In particular, at $t = 8$ μ sec, the cloud had lost about 30% of its energy. In the initial stage, the main energy was transferred to the background ions, as should be the case on retardation via the vortical electric field, with only 5% consumed on changing the magnetic field. There is fairly good agreement between the azimuthal ion currents as shown in Fig. 6 as obtained by experiment (curve 1) and as found by numerical simulation (curve 2), which is important evidence that the cloud-background interaction is due to MLM.

Therefore, these experiments and numerical calculations in good agreement with them show that the magnetic laminar mechanism can provide collisionless energy transfer from a cloud to a background even at $M_A \gg 1$ on a scale of R_m if the value of the universal MLM interaction parameter is sufficiently large ($\delta \gtrsim 1$).

LITERATURE CITED

1. V. F. D'yachenko, V. S. Imshennik, and V. V. Paleichik, "Motion of the interstellar medium produced by the shell of a nova or supernova," *Astron. Zh.*, **46**, No. 4 (1969).
2. The Argus Operation [in Russian], Atomizdat, Moscow (1960).
3. The Sea Star Operation [in Russian], Atomizdat, Moscow (1964).
4. I. O. Bohachevsky, J. C. Goldstein, and D. O. Dickman, "Plasma behaviour in magnetically protected inertial confinement fusion reactor cavities," *Nucl. Technol./Fusion*, **1**, No. 7 (1981).

5. V. M. Antonov, V. P. Bashurin, et al., "Laboratory simulation effects of collisionless interaction in super-Alfvénic space plasma flows," in: Contr. Pap. Int. Conf. on Phenomena in Ionized Gases, Vol. 1, Dusseldorf (1983).
6. C. W. Mendel and T. P. Wright, "Nonturbulent electric fields in soliton and shocklike structures in magnetized plasmas," J. Plasma Phys., 10, Part 1 (1973).
7. J. B. McBride, E. Ott, et al., "Theory and simulation of turbulent heating by the modified two-stream instability," Phys. Fluids, 15, No. 12 (1972).
8. T. P. Wright, "Early-time model of laser plasma expansion," Phys. Fluids, 14, No. 9 (1971).
9. A. I. Golubev, A. A. Solov'ev, and V. A. Terekhin, "Collisionless expansion of an ionized cloud in a homogeneous magnetized plasma," Zh. Prikl. Mekh. Tekh. Fiz., No. 5 (1978).
10. Yu. P. Zakharov and A. G. Ponomarenko, "Collisionless interaction of a flow of laser plasma with a magnetized plasma medium," in: Interaction of Laser Radiation with Matter [in Russian], A. G. Ponomarenko (ed.), ITPM Sib. Otd. Akad. Nauk SSSR, Novosibirsk (1980).
11. V. P. Bashurin, A. I. Golubev, and V. A. Terekhin, "Collisionless retardation of an ionized cloud expanding into a homogeneous magnetized plasma," Zh. Prikl. Mekh. Tekh. Fiz., No. 5 (1983).
12. J. W. M. Paul, C. C. Daughney, et al., "Experimental study of collisionless shock waves," in: Proc. 4th Int. Conf. on Plasma Physics and Contr. Nuclear Fusion Research, V. 111, Madison (1971).
13. V. M. Antonov, L. B. Gevorkyan, et al., "Laboratory simulation of nonstationary processes in solar wind plasma," in: Contr. Papers of the 15th Int. Conf. on Phenomena in Ionized Gases, Part 1, Minsk (1981).
14. V. M. Antonov, L. B. Gevorkyan, et al., "Experimental studies on the interaction of a laser plasma with a magnetic field and a magnetized plasma medium," in: Interaction of Laser Radiation with Matter [in Russian], A. G. Ponomarenko (ed.), ITPM SO AN SSSR, Novosibirsk (1980).
15. A. V. Melekhov, A. M. Orishich, et al., "A high-power CO₂ amplifier for generating plasma clouds," in: Interaction of Laser Radiation with Matter [in Russian], A. G. Ponomarenko (ed.), ITPM SO AN SSSR, Novosibirsk (1980).
16. V. M. Antonov, Yu. P. Zakharov, et al., "An experimental study of stability in the interaction of a spherical laser plasma cloud with a magnetic field," in: Proceedings of the Sixth All-Union Conference on Low-Temperature Plasma Physics [in Russian], Vol. 2, Leningrad (1983).
17. Yu. P. Raizer, "Retardation and energy conversion for a plasma expanding in an empty space containing a magnetic field," Zh. Prikl. Mekh. Tekh. Fiz., No. 6 (1963).
18. V. M. Antonov, Yu. P. Zakharov, V. V. Maksimov, A. M. Orishich, A. G. Ponomarenko, and V. G. Posukh, "A Study of the Conditions for Formation of Laser-Plasma Clouds Containing $N \sim 10^{19}$ Particles with Two-Pulse Target Irradiation [in Russian], Preprint No. 13-84, ITPM SO AN SSSR (1984).